

Susceptibility and specific-heat studies on the directionally anisotropic Heisenberg antiferromagnets

A. N. Das, P. Mandal, P. Choudhury,* and B. Ghosh

Saha Institute of Nuclear Physics, 92 Acharya Prafulla Chandra Road, Calcutta 700 009, India

(Received 9 February 1987; revised manuscript received 29 February 1988)

The high-temperature series for the zero-field susceptibility has been studied for a directionally anisotropic Heisenberg antiferromagnet which has different interactions along different lattice directions (J_1 in the xy plane and RJ_1 along the z direction). With the use of high-temperature series up to five terms, the susceptibility has been found out for $S = \frac{5}{2}$ and 1 systems adopting a graphical extrapolation procedure and a Padé-approximant technique. The reduced temperature $\tau_{\max} = k_B T_{\max} / |J_1| S(S+1)$ at which the maximum in the susceptibility occurs has been evaluated for different R ($-0.6 \leq R \leq 1.0$). The low-temperature behavior of the susceptibility and the magnon specific heat have been studied using the spin-wave theory. The transition temperature of the system for various values of R has been computed using the random-phase-approximation method. The magnetic data of Ba_2NiF_6 system have been compared with the high-temperature series and the spin-wave theory predictions. The best fit is obtained for $R=0.1$ with $J_1 = -37$ K.

I. INTRODUCTION

Many magnetic systems are not directionally isotropic in the sense that the interaction strengths in all lattice directions are not equal.¹ For such anisotropic systems the high-temperature series for the susceptibility and the specific heat have been developed and studied for classical spins ($S = \infty$) only.^{2,3} We consider a model Hamiltonian describing a Heisenberg system with directionally anisotropic interaction

$$\begin{aligned} \mathcal{H} &= -2J_1 \sum_{\langle ij \rangle}^{xy} \mathbf{S}_i \cdot \mathbf{S}_j - 2J_2 \sum_{\langle ij \rangle}^z \mathbf{S}_i \cdot \mathbf{S}_j - g\mu_B H_0 \sum_i S_i^z \\ &= -2J_1 \left[\sum_{\langle ij \rangle}^{xy} \mathbf{S}_i \cdot \mathbf{S}_j + R \sum_{\langle ij \rangle}^z \mathbf{S}_i \cdot \mathbf{S}_j \right] \\ &\quad - g\mu_B H_0 \sum_i S_i^z, \end{aligned} \quad (1)$$

where the first summation is restricted to nearest-neighbor pairs of spins which lie in a common xy plane while the second summation is over nearest-neighbor pairs of spins which lie along a common z direction. The quantity $R = J_2/J_1$ is the ratio of interplanar to intraplanar coupling strengths and is referred to as the anisotropy parameter. We have studied the susceptibility at high and low temperatures and the specific heat at low temperatures of the above model (1), with $J_1 < 0$ (antiferromagnetic interaction) and for various values of R ranging from 1.0 to -1.0 by using the high-temperature series (HTS) expansion method and the spin-wave theory. The transition temperature of the system has been determined using the random-phase-approximation (RPA) method.

Dalton⁴ derived the series expansion for the zero-field susceptibility to order 5 for general spin and general lattice structure for both Heisenberg and Ising systems in which the first- and second-neighbor interactions were included. The main task of the high-temperature series expansion is to calculate the trace of the term

$$\left[\left(\sum_{\langle ij \rangle} J_{ij} \mathbf{S}_i \cdot \mathbf{S}_j \right)^n \sum_i S_i^z \right].$$

The calculation involves determination of number of possible interaction graphs, its occurrence factor, and the trace of each graph. The anisotropic model Hamiltonian (1) considers two types of interactions. For this model, determination of the trace of the term

$$\left[\left(\sum_{\langle ij \rangle} J_{ij} \mathbf{S}_i \cdot \mathbf{S}_j \right)^n \sum_i S_i^z \right]$$

is identical to that of Dalton who also considered two types of interactions. We have used the coefficients derived by Dalton⁴ and calculated the series for the zero-field susceptibility up to five terms for the model system (1), with four nearest neighbors in the xy plane and two along the z direction for $S = \frac{5}{2}$ and 1. The reciprocal susceptibility has been found out adopting extrapolation procedure and Padé-approximant technique for different values of R , hence, the reduced temperatures

$$\tau_{\max} = k_B T_{\max} / |J_1| S(S+1),$$

at which the maxima in susceptibility occur, have been determined.

The low-temperature susceptibility has been found out using Kubo's formula⁵ which relates the susceptibility of the antiferromagnetic system with the spin-wave (magnon) energies. We have determined the spin-wave energies of the system (1) and calculated the zero-field susceptibility and magnon specific heat for various values of R .

From the magnetic behavior of Ba_2NiF_6 Yamaguchi and Sakuraba⁶ inferred that it is a two-dimensional Heisenberg antiferromagnet with large anisotropy. Navarro⁷ mentioned that there is a small three-dimensional (3D) coupling in this compound. We have compared the susceptibility data of Ba_2NiF_6 with the HTS and spin-wave theory predicted results for different values of R and good fit is obtained for $R = 0.1$.

II. HIGH-TEMPERATURE SERIES EXPANSION

Following the moment method of Rushbrooke and Wood⁸ the series for the zero-field susceptibility for our model Hamiltonian (1) is given by

$$\frac{\chi k_B T}{Ng^2 \mu_B^2} = \frac{1}{3} X \left[1 + \sum_{n \geq 1} a_n x^n \right], \quad (2)$$

where $X = S(S+1)$, $x = |J_1| / k_B T$, N is the total number of spins in the system, and

$$a_n = \frac{3}{X} \frac{2^n}{n!} \quad (\text{coefficients of } N \text{ in } \langle P^n Q^2 \rangle), \quad (3)$$

where

$$\langle P^n Q^2 \rangle = \frac{1}{(2S+1)^n} \text{Tr}(P^n Q^2), \quad (4)$$

$$P = \sum_{(ij)}^{xy} \mathbf{S}_i \cdot \mathbf{S}_j + R \sum_{(ij)}^z \mathbf{S}_i \cdot \mathbf{S}_j, \quad Q = \sum_i S_i^z. \quad (5)$$

The calculation of the trace $\langle P^n Q^2 \rangle$ involves determination of the number of possible interaction graphs, each to be multiplied by its occurrence factor in the lattice of N sites and the trace of each graph. Since two types of interactions J_1 and J_2 have been considered, two types of bonds would appear in the interaction graphs which may be conveniently denoted by a light line or a heavy line representing interaction strength J_1 or RJ_1 .⁹ The zero-field susceptibility coefficient a_n , being determined by the n th order interaction graphs is thus a polynomial of degree n in R , since each interaction line may, in principle, be of either type. The series for the susceptibility may be written in the form

$$\frac{\chi k_B T}{Ng^2 \mu_B^2} = \frac{1}{3} X \left[1 + \sum_{r+s \geq 1} a_{rs}(X) R^s x^{r+s} \right]. \quad (6)$$

The coefficients $a_{rs}(X)$, for general spin and general lattice structure have been given by Dalton⁴ for $r+s \leq 5$. He denoted the coefficients by $b_{rs}(X)$, which are related to the coefficients $a_{rs}(X)$, in Eq. (6), by

$$a_{rs}(X) = b_{rs}(X) 2^{-(r+s)}. \quad (7)$$

For our model system (1), the lattice constants, in the notation of Dalton,⁴ are

$$\begin{aligned} q_1 = 4, \quad q_2 = 2, \quad S_1 = 1, \quad S_3 = 2, \\ S_2 = S_4 = 0, \quad T_i = 0, \quad P_i = 0. \end{aligned} \quad (8)$$

Using Eqs. (7) and (8) the coefficients $a_{rs}(X)$ in Eq. (6) have been determined.

The series for the reciprocal susceptibility is obtained from the inverse of Eq. (6)

$$\frac{Ng^2 \mu_B^2}{\chi |J_1|} = 3\tau \left[1 + \sum_{n \geq 1} \frac{b_n}{\tau^n} \right], \quad (9)$$

where $\tau = k_B T / |J_1| S(S+1)$ and the coefficients b_n 's are determined from $a_{rs}(X)$'s for different R values up to $n = 5$. Using this series (9) best theoretical estimates for the reciprocal susceptibility as a function of τ are ob-

tained by plotting $Ng^2 \mu_B^2 / \chi |J_1|$ as a function of $1/n$ and extrapolating graphically to $n = \infty$. The error involved in the extrapolation (with such limited number of terms) is large for temperatures below τ_{\max} at which the maximum in the susceptibility (χ_{\max}) occurs and the extrapolation becomes impossible for $\tau < 0.9\tau_{\max}$.

A standard method in analyzing truncated high-temperature series expansions is the Padé-approximant technique.¹⁰ We have formed Padé approximants (PA's) to the series of Eq. (9). Some representative plots of near diagonal PA's [3,2] and [2,3] along with the curve obtained from graphical extrapolation procedure are shown in Fig. 1. The PA [1,4] curve (not shown) lies in between [3,2] and [2,3] curves. The susceptibility behavior is well established by all the curves for $\tau > 1.25\tau_{\max}$, whereas below this we take the average of [2,3] curve and the extrapolated curve as a reasonable prediction¹¹ for the reciprocal susceptibility. Because of the limited number of terms in Eq. (9) prediction of χ becomes unreliable below τ_{\max} .

Some representative plots of $\chi |J_1| / Ng^2 \mu_B^2$ against τ are shown in Fig. 2 for $S = \frac{5}{2}$. From such plots the value of τ_{\max} and the maximum value of the reduced susceptibility $\chi_{\max} |J_1| / Ng^2 \mu_B^2$ have been evaluated. The values are given in Table I for various values of R and for $S = \frac{5}{2}$ and 1.

Limited number of terms in Eq. (9) produce an uncertainty in τ_{\max} . When our results of τ_{\max} are compared with those obtained by de Jongh¹² and Lines¹³ for $R = 0$ and 1.0 systems, it is found that τ_{\max} , evaluated by us, is within $\pm 5\%$ of their values for $S = \frac{5}{2}$ and the difference is

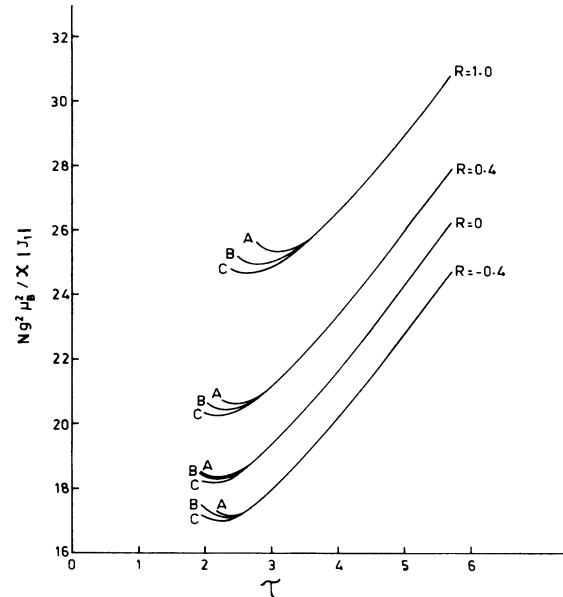


FIG. 1. Theoretical predictions for the reciprocal susceptibility of a directionally anisotropic Heisenberg antiferromagnet ($S = \frac{5}{2}$) for various values of R ($=J_2/J_1$), as obtained from the high-temperature series, against reduced temperature $\tau = k_B T / |J_1| S(S+1)$. Curve A is obtained adopting extrapolation procedure, B and C are [2,3] and [3,2] PA curves, respectively.

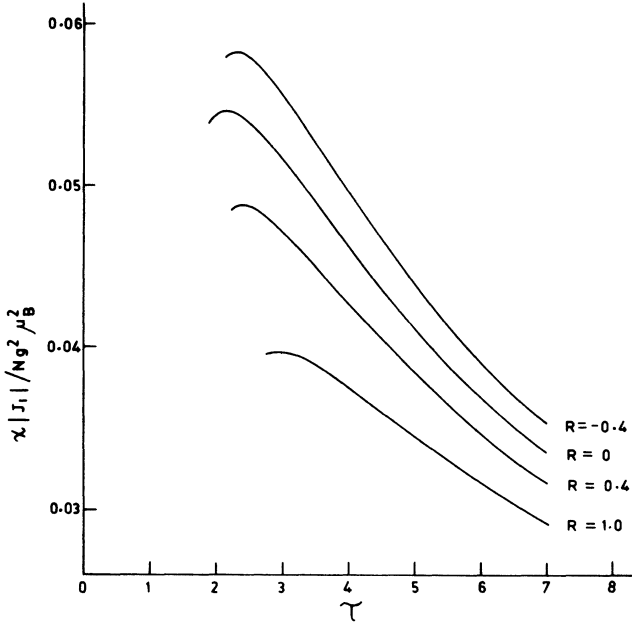


FIG. 2. Predictions for the susceptibility against reduced temperature for $S = \frac{5}{2}$ and for several values of R .

less than 2% for $S=1$. The error in estimating $\bar{\chi}_{\max}$ is much smaller ($\sim 1\%$) since the value of $\bar{\chi}_{\max}$ can be determined with a greater accuracy from the finite number of terms known in the series.

In Fig. 3 we have plotted the reduced susceptibility $\chi \Theta_{\text{MF}}/C$ against T/Θ_{MF} for $S = \frac{5}{2}$, where Θ_{MF} is the molecular field Curie-Weiss temperature,

$$\Theta_{\text{MF}} = 2(4 + 2R)S(S + 1) |J_1| / 3k_B.$$

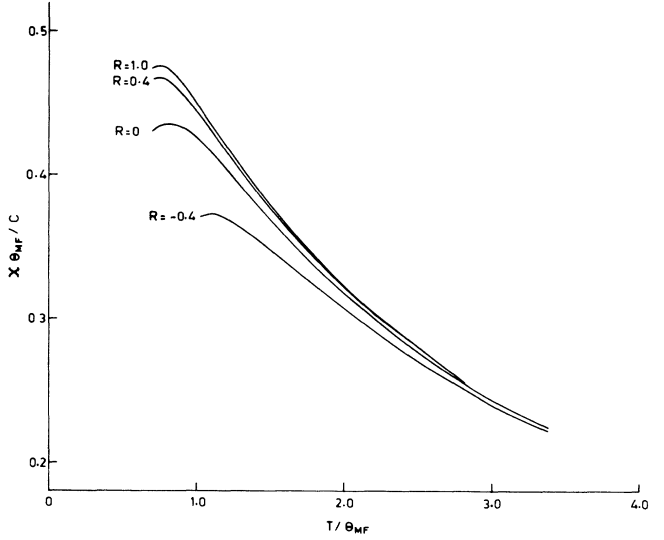


FIG. 3. Plot of $\chi \Theta_{\text{MF}}/C$ vs T/Θ_{MF} for $S = \frac{5}{2}$, where C is Curie constant and Θ_{MF} is the molecular field Curie-Weiss temperature.

Using these reduced units, the variation of the effective number of magnetic neighbors with the anisotropy parameter (R) is accounted for and these plots appear to be more useful for comparison for $R \geq 0$.¹¹ Inspection of these curves (Fig. 3) shows that for $T/\Theta_{\text{MF}} > 1.2$ the susceptibility of $R = 0.4$ system differs by less than 1% from the corresponding value for $R = 1.0$ and even at T_{\max} the difference is about 1.5%.

We have also determined the reduced Curie-Weiss tem-

TABLE I. Estimated values for $\tau_{\max} = k_B T_{\max} / |J_1| S(S + 1)$, $\bar{\chi}_{\max} = \chi_{\max} |J_1| / Ng^2 \mu_B^2$, $\chi_{\max} T_{\max} / C$ [$C = Ng^2 \mu_B^2 S(S + 1) / 3k_B$], $\tau_{\text{CW}} = k_B T_{\text{CW}} / |J_1| S(S + 1)$ (obtained from linear fit of the HTS results of χ^{-1} in the $5\tau_{\max} - 6\tau_{\max}$ region), and the ratio of $\tau_{\text{CW}}/\tau_{\max}$ ($= T_{\text{CW}}/T_{\max}$). Errors involved in the predictions are discussed in the text.

R	τ_{\max}	$\bar{\chi}_{\max}$	$\chi_{\max} T_{\max} / C$	τ_{CW}	T_{CW} / T_{\max}
$S = \frac{5}{2}$					
1.0	2.95	0.0398	0.352	4.453	1.51
0.8	2.75	0.0427	0.352	4.163	1.51
0.6	2.55	0.0458	0.351	3.884	1.52
0.4	2.40	0.0487	0.351	3.599	1.50
0.2	2.25	0.0518	0.350	3.324	1.47
0.0	2.14	0.0545	0.349	3.046	1.42
-0.2	2.25	0.0564	0.381	2.784	1.24
-0.4	2.30	0.0582	0.401	2.517	1.09
-0.6	2.45	0.0595	0.437	2.259	0.92
$S = 1$					
1.0	3.0	0.0383	0.345	4.559	1.52
0.8	2.8	0.0410	0.344	4.263	1.52
0.6	2.6	0.0441	0.344	3.981	1.53
0.4	2.45	0.0468	0.344	3.687	1.51
0.2	2.32	0.0494	0.344	3.416	1.47
0.0	2.22	0.0517	0.344	3.134	1.41
-0.2	2.32	0.0535	0.372	2.872	1.24
-0.4	2.42	0.0549	0.398	2.602	1.08

perature $\tau_{CW} = k_B T_{CW} / |J_1| S(S+1)$ from a linear fit of the χ^{-1} values (HTS predicted) in the high-temperature region. The value of τ_{CW} depends on the temperature range used and decreases at a higher-temperature range [for example, for $R=0$ and $S=\frac{5}{2}$ system τ_{CW} determined from $(3\tau_{\max}-4\tau_{\max})$, $(4\tau_{\max}-5\tau_{\max})$, and $(5\tau_{\max}-6\tau_{\max})$ regions are 3.345, 3.154, and 3.046, respectively]. The values of τ_{CW} , determined from $5\tau_{\max}-6\tau_{\max}$ region, and the ratio (τ_{CW}/τ_{\max}) for various values of R are also given in Table I.

The values of τ_{\max} and $\chi_{\max} T_{\max}/C$ are minimum for $R=0$ and increase as $|R|$ increases. For $R < 0$ (when the ferromagnetic interaction is introduced along the z direction) the value of $\chi_{\max} T_{\max}/C$ shows a rapid increase while T_{CW}/T_{\max} shows a rapid fall with increase of $|R|$. Puertolas *et al.*³ studied a similar anisotropic Heisenberg system for $S = \infty$ using a longer series and obtained similar behavior. Apart from some quantitative difference our results for $S = \frac{5}{2}$ are in agreement with those of Puertolas *et al.*³ for $S = \infty$ (after necessary scaling).

III. ORDERED PHASE: SPIN-WAVE THEORY

The Hamiltonian (1), describing antiferromagnetic interactions among the spins on the xy plane and either antiferromagnetic ($R > 0$) or ferromagnetic ($R < 0$) interactions along the z direction, has two ordered antiferromagnetic solutions. For $R > 0$, a spin belonging to sublattice a has six neighbors with antiparallel spin which form sublattice b and vice versa. For $R < 0$, a spin on sublattice a has four neighbors on the xy plane with antiparallel spin which belong to sublattice b and two neighbors along the z direction with parallel spin, belonging to sublattice a . The spin arrangements are shown in Fig. 4.

Using the Holstein-Primakoff transformation to map the spin deviations to the bosonic space (free magnon) and applying the usual Fourier transformation to the momentum (\mathbf{k}) space, the Hamiltonian (1) may be expressed in terms of creation and annihilation operators for both sublattices, which after diagonalization¹⁴ reduces to

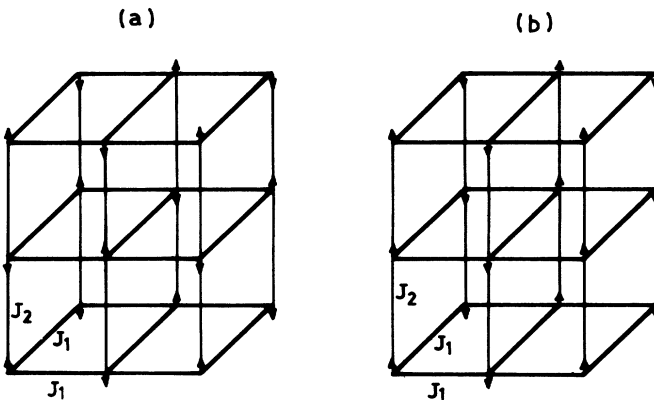


FIG. 4. Spin arrangement of the ordered state: (a) $R > 0$ and (b) $R < 0$.

$$\mathcal{H} = C_2 - \sum_{\mathbf{k}} A_{\mathbf{k}} + \sum_{\mathbf{k}} (\alpha_{\mathbf{k}}^\dagger \alpha_{\mathbf{k}} + \frac{1}{2}) \times [(A_{\mathbf{k}}^2 - |B_{\mathbf{k}}|^2)^{1/2} + H_{\mathbf{k}}] + \sum_{\mathbf{k}} (\beta_{\mathbf{k}}^\dagger \beta_{\mathbf{k}} + \frac{1}{2}) [(A_{\mathbf{k}}^2 - |B_{\mathbf{k}}|^2)^{1/2} - H_{\mathbf{k}}], \quad (10)$$

where

$$C_2 = -2Ng\mu_B SH_A - NS(J_0^{aa} + J_0^{bb} - 2J_0^{ab}), \quad (11)$$

$$H_{\mathbf{k}} = g\mu_B H_0,$$

$$A_{\mathbf{k}} = g\mu_B H_A + J_0^{aa} - J_0^{ab} - J_{\mathbf{k}}^{aa},$$

and

$$B_{\mathbf{k}} = -J_{\mathbf{k}}^{ab}.$$

H_A is the anisotropic field which exists in real antiferromagnetic systems:

$$J_{\mathbf{k}}^{aa} = 2S \sum_{l'} J_{ll'} \exp(i\mathbf{k} \cdot \mathbf{r}_{ll'}), \quad (13)$$

$$J_{\mathbf{k}}^{bb} = 2S \sum_{m'} J_{mm'} \exp(i\mathbf{k} \cdot \mathbf{r}_{mm'}), \quad (14)$$

$$J_{\mathbf{k}}^{ab} = 2S \sum_m J_{lm} \exp(i\mathbf{k} \cdot \mathbf{r}_{lm}), \quad (15)$$

where l, l' denote lattice sites of a sublattice and m, m' those of b sublattice.

Case A: $R > 0$. The ordered state spin arrangement is shown in Fig. 4(a) and for this case

$$J_{\mathbf{k}}^{aa} = J_{\mathbf{k}}^{bb} = 0, \quad (16)$$

and

$$J_{\mathbf{k}}^{ab} = -4S |J_1| (\cos k_x a + \cos k_y a + R \cos k_z c). \quad (17)$$

The magnon energy, in absence of any external field, is obtained as

$$\begin{aligned} \hbar\omega_{\mathbf{k}} &= (A_{\mathbf{k}}^2 - |B_{\mathbf{k}}|^2)^{1/2} \\ &= 8S |J_1| [(1+R/2)^2(1+\alpha)^2 \\ &\quad - \frac{1}{4}(\cos k_x a + \cos k_y a + R \cos k_z c)^2]^{1/2}, \end{aligned} \quad (18)$$

where

$$\alpha = g\mu_B H_A / 8S |J_1| (1+R/2). \quad (19)$$

Case B: $R < 0$. For this case, the ordered state spin arrangement is shown in Fig. 4(b) and

$$J_{\mathbf{k}}^{aa} = J_{\mathbf{k}}^{bb} = 4SJ_2 \cos k_z c, \quad (20)$$

$$J_{\mathbf{k}}^{ab} = -4S |J_1| (\cos k_x a + \cos k_y a). \quad (21)$$

The magnon energy is given by

$$\begin{aligned} \hbar\omega_{\mathbf{k}} &= 8S |J_1| \left[\left(\left[1 + |R| \sin^2 \frac{k_z c}{2} + \alpha \right]^2 \right. \right. \\ &\quad \left. \left. - \frac{1}{4}(\cos k_x a + \cos k_y a)^2 \right)^{1/2} \right], \end{aligned} \quad (22)$$

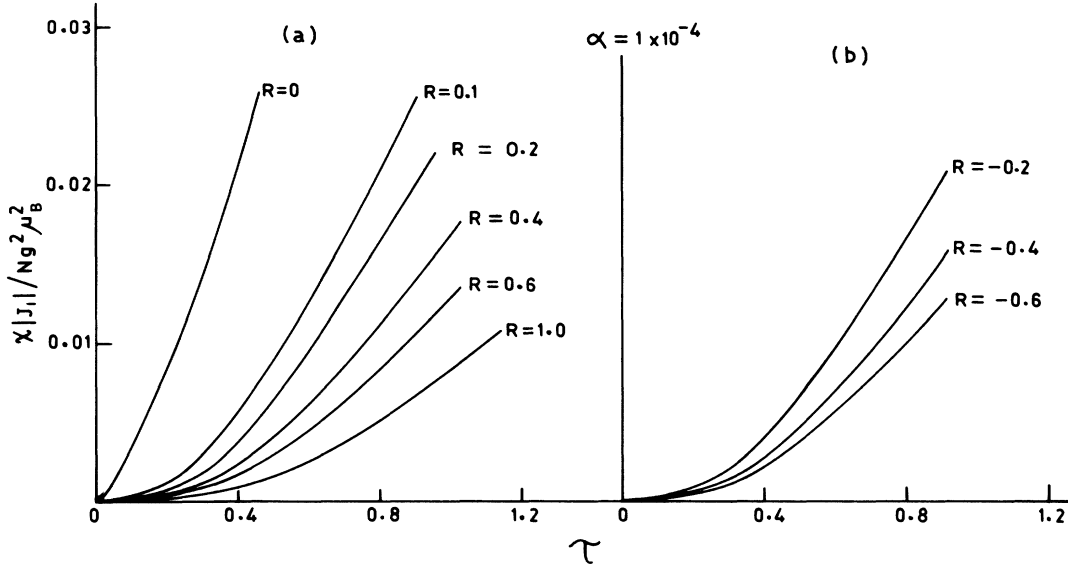


FIG. 5. Susceptibility, calculated from the spin-wave theory, against reduced temperature for $S = \frac{5}{2}$. (a) $R > 0$; (b) $R < 0$.

where

$$\alpha = g\mu_B H_A / 8S |J_1|. \quad (23)$$

The zero-field parallel susceptibility in terms of magnon energy is given by⁵

$$\frac{\chi_{\parallel}}{Ng^2\mu_B^2} = \frac{2}{k_B T} \frac{1}{N} \sum_{\mathbf{k}} \frac{e^{\hbar\omega_{\mathbf{k}}/k_B T}}{(e^{\hbar\omega_{\mathbf{k}}/k_B T} - 1)^2}, \quad (24)$$

where the summation is taken over $N/2$ points in the Brillouin zone.

Using Eqs. (18), (22), and (24) we have calculated the reduced susceptibility $\chi_{\parallel} |J_1| / Ng^2\mu_B^2$ in terms of reduced temperature τ for $S = \frac{5}{2}$, $\alpha = 1 \times 10^{-4}$, and R ranging from -1.0 to $+1.0$. The plots of the reduced susceptibility versus τ are shown in Fig. 5. In Fig. 6 we have shown the corresponding plots for $S = 1$ and $\alpha = 0.03$.

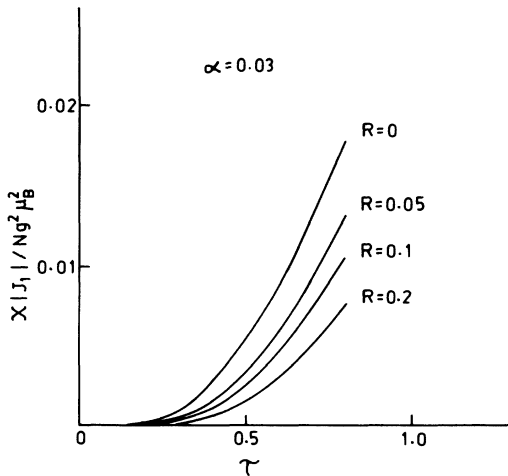


FIG. 6. Susceptibility, calculated from the spin-wave theory, against reduced temperature for $S = 1$.

The magnon specific heat in absence of any external field is given by the relation

$$\frac{C_m}{R} = \frac{2}{N} \sum_{\mathbf{k}} \left[\frac{\hbar\omega_{\mathbf{k}}}{k_B T} \right]^2 \frac{e^{\hbar\omega_{\mathbf{k}}/k_B T}}{(e^{\hbar\omega_{\mathbf{k}}/k_B T} - 1)^2}. \quad (25)$$

The summation is taken over $N/2$ points in the Brillouin zone. The specific heat for different R values has been calculated using Eqs. (18), (22), and (25) for $S = \frac{5}{2}$ only. The plots of the specific heat versus τ for various values of R are shown in Fig. 7.

In Fig. 8 we have plotted $\chi\Theta_{MF}/C$ against T/Θ_{MF} at low temperatures for different positive values of R . As mentioned earlier these plots for $R > 0$ would be more useful for comparison.

IV. RANDOM-PHASE GREEN'S FUNCTION APPROXIMATION

The high-temperature series that we have considered has only five terms and can describe the susceptibility down to τ_{\max} . Exact prediction of χ below τ_{\max} and determination of the transition temperature (T_c) requires a much longer series. The spin-wave theory can describe the system in the temperature range $0 \leq T \leq T_c/2$. So for determination of the transition temperature of the anisotropic system we take recourse to the random-phase approximation.

The double-time Green's function of Heisenberg operators $A(t)$ and $B(t')$ is defined as

$$\langle\langle A(t); B(t') \rangle\rangle = -i\Theta(t-t') \langle [A(t), B(t')]_- \rangle. \quad (26)$$

The Fourier transform of (26)

$$\langle\langle A; B \rangle\rangle^{(\omega)} = \int_{-\infty}^{+\infty} \langle\langle A(t); B(t') \rangle\rangle e^{i\omega(t-t')} d(t-t')$$

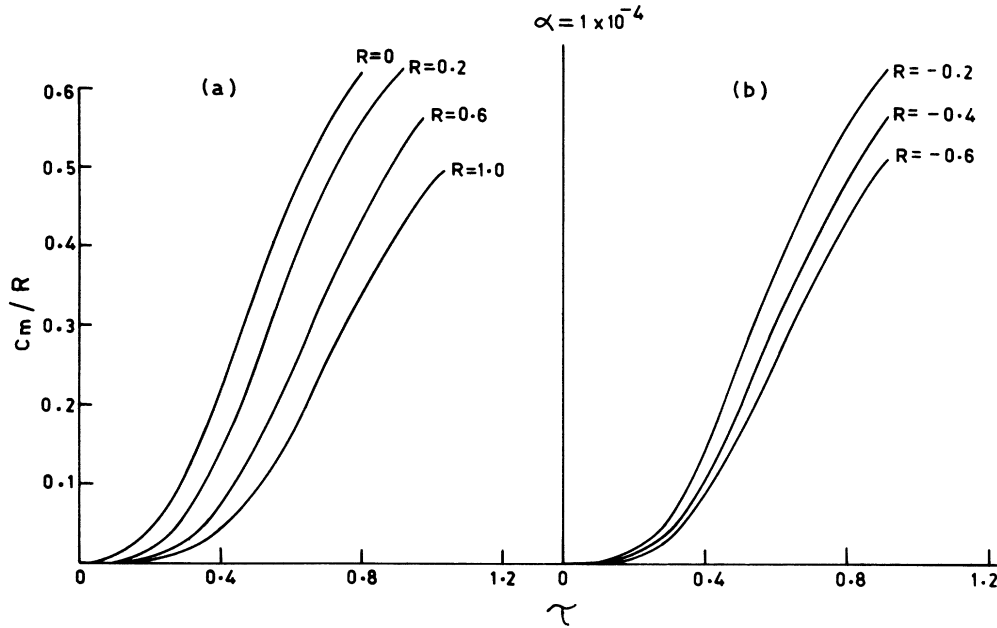


FIG. 7. Magnon specific heat, obtained from the spin-wave theory, against reduced temperature: (a) $R > 0$ and (b) $R < 0$ ($S = \frac{5}{2}$).

satisfies the equation of motion

$$\omega \langle\langle A; B \rangle\rangle^{(\omega)} = \langle [A, B]_- \rangle + \langle\langle [A, \mathcal{H}]_-; B \rangle\rangle^{(\omega)}. \quad (27)$$

The Hamiltonian of the Heisenberg system in the presence of a small anisotropy field H_A is given by

$$\mathcal{H} = -2 \sum_{\langle ij \rangle} J_{ij} \mathbf{S}_i \cdot \mathbf{S}_j - \sum_{i=1} g \mu_B H_A S_i^z + \sum_{j=1} g \mu_B H_A S_j^z. \quad (28)$$

Choosing the operators $A = S_i^+$ and $B = f(S_h^-) S_h^-$ the equation of motion of the Green's function is

$$\begin{aligned} \omega \langle\langle S_i^+; B \rangle\rangle^{(\omega)} &= \langle [S_i^+, B]_- \rangle \\ &- \sum_{j=i} 2J_{ij} \langle\langle (S_j^+ S_i^z - S_i^+ S_j^z); B \rangle\rangle^{(\omega)} \\ &+ g \mu_B H_A \sigma \langle\langle S_i^+; B \rangle\rangle^{(\omega)}, \end{aligned} \quad (29)$$

where $\sigma = 1(-1)$ for site i is occupied by up (down) spin. In the random-phase approximation the higher-order Green's function is decoupled in the form

$$\langle\langle S_j^+ S_i^z; B \rangle\rangle = \langle S_i^z \rangle \langle\langle S_j^+; B \rangle\rangle. \quad (30)$$

At low temperatures the ordered spin structure (Fig. 4) is such that the lattice can be subdivided into two translationally invariant sublattices, the "up" and the "down" with average value of spin per site \bar{S} and $-\bar{S}$, respectively. Choosing h to be a site occupied by an up spin, when i and h are on the same sublattice one can define the Fourier transform with respect to the reciprocal sublattice

$$G_{1\mathbf{k}}(\omega) = \sum_{i-h} \langle\langle S_i^+; B \rangle\rangle^{(\omega)} \exp[-i\mathbf{k} \cdot (\mathbf{i} - \mathbf{h})], \quad (31)$$

$$\langle\langle S_i^+; B \rangle\rangle^{(\omega)} = \frac{2}{N} \sum_{\mathbf{k}} G_{1\mathbf{k}}(\omega) \exp[i\mathbf{k} \cdot (\mathbf{i} - \mathbf{h})], \quad (32)$$

where N is the total number of spins in the lattice and \mathbf{k} is a reciprocal lattice vector which runs over $N/2$ points in the first Brillouin zone of the reciprocal sublattice. In an exact way $G_{2\mathbf{k}}$ is defined for the case where i and h are on the opposite sublattice.

To find out the transition temperature of the system (28) for general S , it is sufficient to choose $f(S_h^-) = 1$, i.e., $B = S_h^-$. Following Lines¹⁵ the equation of motion of the two Green's functions are derived as

$$(\omega - g \mu_B H_A + \bar{S} \mu) G_{1\mathbf{k}}(\omega) = 2\bar{S} - \bar{S} \lambda G_{2\mathbf{k}}(\omega), \quad (33)$$

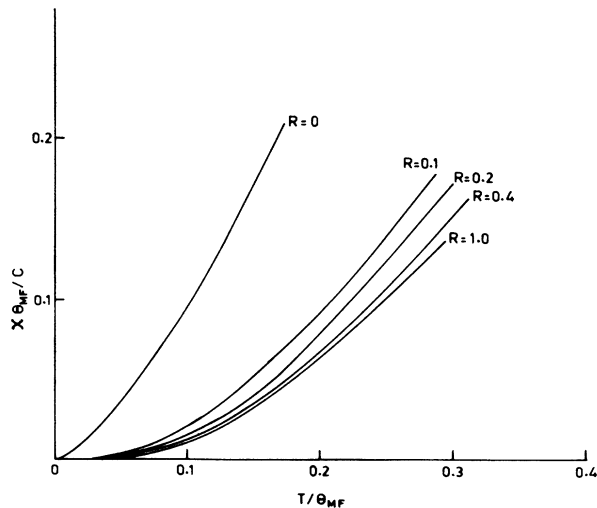


FIG. 8. Plot of $\chi \Theta_{MF} / C$ against T / Θ_{MF} in the low-temperature region for $S = \frac{5}{2}$.

$$(\omega + g\mu_B H_A - \bar{S}\mu)G_{2k}(\omega) = \bar{S}\lambda G_{1k}(\omega), \quad (34)$$

where

$$\mu = \sum_{i-j}^s 2J_{ij} \{ \exp[-i\mathbf{k}\cdot(\mathbf{i}-\mathbf{j})] - 1 \} + \sum_{i-j}^d 2J_{ij}, \quad (35)$$

$$\langle S_h^-(t') S_i^+(t) \rangle = \frac{2}{N} \sum_{\mathbf{k}} \exp[i\mathbf{k}\cdot(\mathbf{i}-\mathbf{h})] \cdot \lim_{\epsilon \rightarrow 0^+} i \int_{-\infty}^{\infty} \frac{G_{1k}(\omega + i\epsilon) - G_{1k}(\omega - i\epsilon)}{e^{\hbar\omega/k_B T} - 1} e^{-i\omega(t-t')} d\omega. \quad (37)$$

For the case $t = t'$ and $i = h$

$$\langle S_h^- S_h^+ \rangle = \bar{S} \left\langle \left[-\frac{A}{E_0} \coth(E_0 \bar{S} / 2k_B T) \right]_{\mathbf{k}} - 1 \right\rangle, \quad (38)$$

where

$$A = \mu - g\mu_B H_A / \bar{S}, \quad (39)$$

$$E_0 = (A^2 - \lambda^2)^{1/2}.$$

$\langle \rangle_{\mathbf{k}}$ indicates an average of \mathbf{k} over $N/2$ values in the first Brillouin zone of the reciprocal sublattice.

At and above the transition temperature (T_c), $\langle S_x^2 \rangle = \langle S_y^2 \rangle = \langle S_z^2 \rangle = S(S+1)/3$ and as $T \rightarrow T_c$ from below, $\bar{S} \rightarrow 0$ and it follows

$$\frac{S(S+1)}{3k_B T_c} = \left\langle -\frac{A}{E_0^2} \right\rangle_{\mathbf{k}}. \quad (40)$$

Case I: $R > 0$, the ordered spin arrangement is shown in Fig. 4(a) and for this case

$$\mu = -4 |J_1| (2+R), \quad (41)$$

$$\lambda = -4 |J_1| [\cos(k_x a) + \cos(k_y a) + R \cos(k_z c)]. \quad (42)$$

The expression for T_c comes out as

$$I_2 = \left\langle \left[\frac{1 + |R| \sin^2(k_z c / 2) + \alpha}{\{ [1 + |R| \sin^2(k_z c / 2) + \alpha]^2 - \frac{1}{4} [\cos(k_x a) + \cos(k_y a)]^2 \}} \right]_{\mathbf{k}} \right\rangle, \quad (49)$$

$$\alpha = g\mu_B H_A / 8 |J_1| \bar{S}. \quad (50)$$

Within the Green's function approximation the anisotropy H_A is assumed as if proportional to \bar{S} so that α is temperature independent.¹³ Using Eqs. (43), (44), (48), and (49) the transition temperature (T_c) has been computed for different values of R ; the curves for T_c are shown in Fig. 9 for positive values of R . For negative values of R , the RPA predicted T_c is less than the corresponding value for positive R . The difference is very small for small anisotropic field (α) and it increases with increasing α and $|R|$. In Table II we have presented the values of $\tau_c = [k_B T_c / |J_1| S(S+1)]$ for positive and negative R values for $\alpha = 4 \times 10^{-4}$ and 2×10^{-1} for comparison.

V. ANALYSIS OF THE SUSCEPTIBILITY OF Ba_2NiF_6

The magnetic susceptibility of Ba_2NiF_6 was measured by Yamaguchi and Sakuraba.⁶ According to them the

$$\lambda = 2 \sum_{i-j}^d J_{ij} \exp[-i\mathbf{k}\cdot(\mathbf{i}-\mathbf{j})]. \quad (36)$$

Solving G_{1k} from Eqs. (33) and (34) the associated correlation function $\langle S^-(t') S^+(t) \rangle$ is determined using the relation

$$\frac{k_B T_c}{S(S+1)} = \frac{1}{3} \frac{8 |J_1|}{(1+\alpha)(1+R/2)} \frac{1}{I_1}, \quad (43)$$

where

$$I_1 = \left\langle \{ (1+R/2)^2 (1+\alpha)^2 - \frac{1}{4} [\cos(k_x a) + \cos(k_y a) + R \cos(k_z c)]^2 \}^{-1} \right\rangle_{\mathbf{k}}, \quad (44)$$

$$\alpha = g\mu_B H_A / 8 |J_1| \bar{S} (1+R/2). \quad (45)$$

Case II: $R < 0$, the ordered spin arrangement is shown in Fig. 4(b) and for this case

$$\mu = -8 |J_1| [1 + |R| \sin^2(k_z c / 2)], \quad (46)$$

$$\lambda = -4 |J_1| [\cos(k_x a) + \cos(k_y a)]. \quad (47)$$

The transition temperature is

$$\frac{k_B T_c}{S(S+1)} = \frac{1}{3} \frac{8 |J_1|}{I_2}, \quad (48)$$

where

system is an example of two-dimensional Heisenberg anti-ferromagnet with large anisotropy ($\alpha \simeq 0.03$), the transition temperature is 93.0 ± 0.5 K and $T_{\max} \sim 165$ K. Navarro⁷ mentioned that the susceptibility data of Ba_2NiF_6 fit with the high-temperature-series predictions for a two-dimensional system, with the values $|J_1| = 38$ K, $g_{\parallel} = 2.23$, $g_{\perp} = 2.10$, and the temperature independent susceptibility $\chi_{\text{tip}} = 1.2 \times 10^{-6}$ emu/g. He has also suggested that there is a small 3D coupling in the system. We have compared the susceptibility data of Ba_2NiF_6 in the paramagnetic region with the HTS predictions and at low temperatures with the spin-wave theory values ($S=1$, $\alpha=0.03$) for $R=0, 0.1$, and 0.2 . The susceptibility (χ_{\parallel}) of Ba_2NiF_6 shows maximum in the temperature range 165–170 K and we have taken $T_{\max} = 167$ K and determined the corresponding values of $|J_1|$ for $R=0, 0.1$, and 0.2 , using the values of τ_{\max} , theoretically pre-

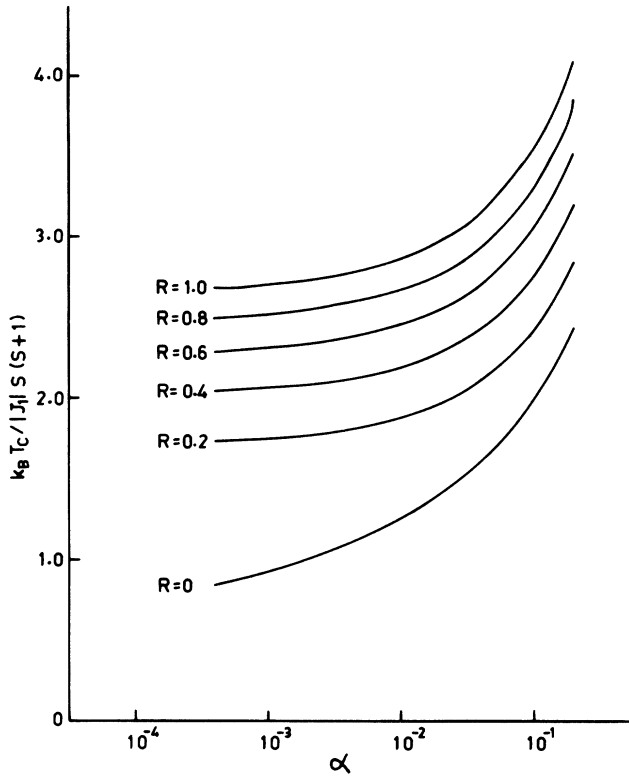


FIG. 9. The transition temperature $[k_B T_c / |J_1| S(S+1)]$ as a function of anisotropy $\alpha [=g\mu_B H_A / 2 |J_1| S(4+2R)]$ for several values of R of a directionally anisotropic Heisenberg antiferromagnet calculated in the RPA Green's function approximation.

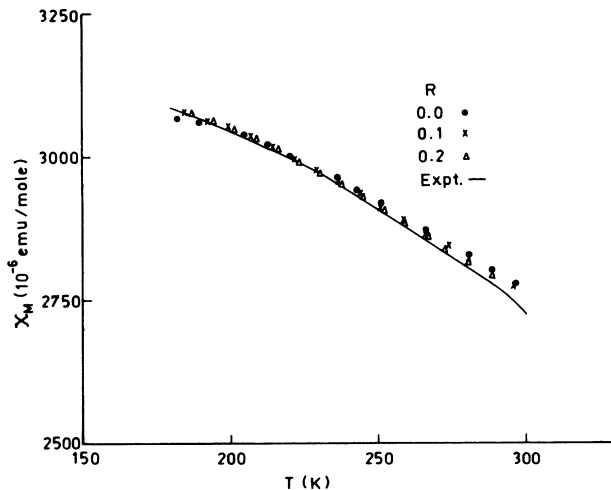


FIG. 10. Comparison of the experimental susceptibility (χ_{\parallel}) of Ba_2NiF_6 ($S=1$) with theoretical HTS predictions for $R=0$, 0.1, and 0.2, corresponding values of $|J_1|$ are 38, 37, and 36 K, respectively. $g_{\parallel}=2.23$ and the temperature independent susceptibility $\chi_{\text{tip}}=536.9 \times 10^{-6}$ emu/mole. Experimental curve is shown by the solid line.

TABLE II. Values of transition temperatures $\tau_c = k_B T_c / S(S+1) |J_1|$, for positive and negative values of R and for $\alpha=4 \times 10^{-4}$ and 2×10^{-1} .

$ R $	$\alpha=4 \times 10^{-4}$		$\alpha=2 \times 10^{-1}$	
	$R > 0$ τ_c	$R < 0$ τ_c	$R > 0$ τ_c	$R < 0$ τ_c
0.0	0.845	0.845	2.431	2.431
0.2	1.732	1.730	2.848	2.775
0.4	2.042	2.039	3.196	3.055
0.6	2.284	2.796	3.511	3.300
0.8	2.492	2.486	3.804	3.523
1.0	2.679		4.082	

dicted. The susceptibility (χ_{\parallel}) of Ba_2NiF_6 and the HTS predictions in the paramagnetic region are shown in Fig. 10 and the spin-wave theory values at low temperatures in Fig. 11. From these plots it is seen that the χ data of Ba_2NiF_6 fit much better with the predictions for $R=0.1$ than those for $R=0$. For this fit we have taken $\chi_{\text{tip}}=1.2 \times 10^{-6}$ emu/g = 536.9×10^{-6} emu/mole, as mentioned by Navarro.⁷

The transition temperature of Ba_2NiF_6 is 93 K. τ_c values from the RPA for $R=0$ and 0.1 ($\alpha=0.03$) are 1.52 and 1.80, respectively. For $S=1$, the RPA value for the transition temperature is very close to T_c observed experimentally for $\alpha=2 \times 10^{-3}$ and for higher values of α the RPA values are lower than those observed experimentally for two-dimensional systems.¹² From the curves given by de Jongh and Miedema¹² it appears that the ratio $(T_c)_{\text{expt}} / (T_c)_{\text{RPA}}$ for $\alpha=0.03$ is 0.73. When this factor is multiplied with the corresponding RPA results (Fig. 9), the transition temperatures for $R=0, 0.1$, and 0.2 systems are 84.3, 97.2, and 107.2 K, respectively. The transition temperature of Ba_2NiF_6 (93 K) is closer to T_c

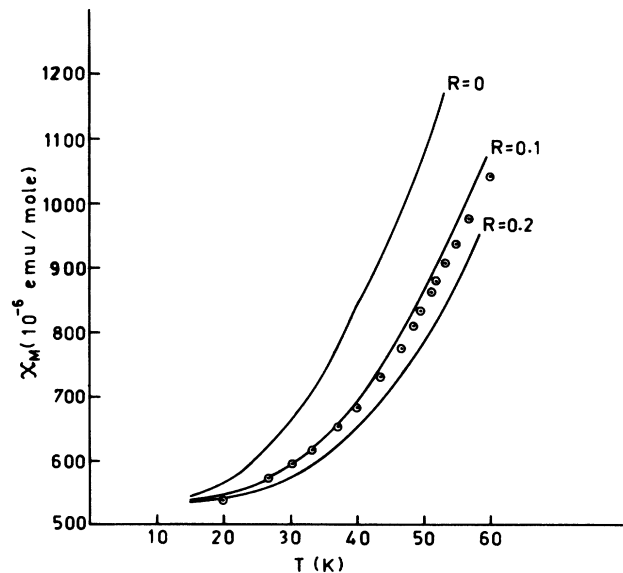


FIG. 11. Comparison of the susceptibility (χ_{\parallel}) of Ba_2NiF_6 with the spin-wave theory predictions at low temperatures ($S=1$, $\alpha=0.03$). g_{\parallel} and χ_{tip} values are given in Fig. 10 (\odot , experimental points).

of $R = 0.1$. So analysis of high- and low-temperature susceptibilities and the transition temperature reveals that Ba_2NiF_6 has a 3D coupling with $R \simeq 0.1$.

VI. DISCUSSION

From the values of $\chi_{\max} T_{\max}/C$, T_{CW}/T_{\max} and plots of reduced susceptibility for $T > T_{\max}$ (Fig. 3) it is seen the χ behavior does not differ by more than 1.5% for $0.4 \leq R \leq 1.0$. We have evaluated the ratio T_{\max}/T_c , determined by the RPA, for various values of R . For $\alpha = 2 \times 10^{-3}$ (for which the RPA results of T_c are close to those observed experimentally for $S = 1$ and $\frac{5}{2}$ systems¹²) T_{\max}/T_c for $S = 1$ are 1.10, 1.13, and 1.17 for $R = 1.0$, 0.5, and 0.4, respectively, and for $R < 0.4$ the ratio increases at a faster rate. A 3–4% change in (T_{\max}/T_c) as R varies from 1.0 to 0.5 is observed for other values of the anisotropy also and for $S = \frac{5}{2}$ the change is even smaller. Puertolas *et al.*³ derived τ_{\max} and τ_c values for classical Heisenberg directionally anisotropic model using a longer series. The ratio of T_{\max}/T_c , in their case, remains almost constant as long as $0.5 \leq R \leq 1.0$.

Figure 8 shows that the susceptibility data at low temperatures for $R = 0.4$ and 1.0 do not differ by more than 8% while for low values of R the difference in susceptibility for different R values is much more. Therefore, it would be difficult to determine the value of R from the susceptibility study alone if it lies between 0.5 and 1.0.

Neutron diffraction, which directly measures the dispersion of magnon energy, would obviously be the most useful tool to determine R in the above case. In the case R lies between 0 and 0.5, fit to the low-temperature susceptibility results would be useful to determine the value of R . This has been manifested when we compare the results of Ba_2NiF_6 with the HTS and spin-wave theory predictions. In the paramagnetic region points for different R values are very close (e.g., the difference in susceptibility for $R = 0.1$ and 0.2 is within 0.3%), while in the low temperature (Fig. 11) the difference is much larger.

For $R < 0$, the value of $\chi_{\max} T_{\max}/C$ increases rapidly and T_{CW}/T_{\max} decreases with increase of $|R|$. So for $R < 0$, the high-temperature susceptibility results are sufficient to determine the value of R .

Finally, from comparison of the susceptibility data of Ba_2NiF_6 with the HTS and the spin-wave theory predicted values it is concluded that this system has a three-dimensional coupling (J_2) and the values of J_1 and J_2 are about 37 and 3.7 K, respectively.

ACKNOWLEDGMENTS

We are grateful to Professor J. Oitmaa, Professor M. Ferer, and Professor L. J. de Jongh for valuable suggestions, encouragement, and communicating some of their results before publication.

*Present address: Central Glass and Ceramic Research Institute, 196 Raja Subodh Chandra Mullick Road, Calcutta 700032, India.

¹L. L. Liu and H. E. Stanley, Phys. Rev. B **8**, 2279 (1973).

²D. N. Lambeth and H. E. Stanley, Phys. Rev. B **12**, 5302 (1975).

³J. A. Puertolas, R. Navarro, F. Palacio, J. Bartolome, D. Gonzalez, and R. L. Carlin, J. Magn. Mater. **31–34**, 1243 (1983); Phys. Rev. B **31**, 516 (1985).

⁴N. W. Dalton, Proc. Phys. Soc. London **88**, 659 (1966).

⁵R. Kubo, Phys. Rev. **87**, 568 (1952).

⁶Y. Yamaguchi and T. Sakuraba, J. Phys. Soc. Jpn. **34**, 834 (1973).

⁷R. Navarro (private communication).

⁸G. S. Rushbrooke and P. J. Wood, Mol. Phys. **1**, 257 (1958); **6**, 409 (1963).

⁹G. S. Rushbrooke, G. A. Baker, and P. J. Wood, in *Phase*

Transitions and Critical Phenomena, edited by C. Domb and M. S. Green (Academic, New York, 1974), Vol. 3, p. 245.

¹⁰D. L. Hunter and G. A. Baker, Phys. Rev. B **7**, 3346 (1973).

¹¹R. Navarro, J. J. Smit, L. J. de Jongh, W. J. Crama, and D. J. W. Ijdo, Phys. **83B**, 97 (1976).

¹²L. J. de Jongh, in *Magnetism and Magnetic Materials, 1972 (Denver)*, Proceedings of the 18th Annual Conference on Magnetism and Magnetic Materials, AIP Conf. Proc. No. **10**, edited by C. D. Graham and J. J. Rhyne (AIP, New York, 1973), p. 561; L. J. de Jongh and A. R. Miedema, Adv. Phys. **23**, 1 (1974).

¹³M. E. Lines, J. Phys. Chem. Solids **31**, 101 (1970); Phys. Rev. **164**, 736 (1967).

¹⁴F. Keffer, in *Handbuch der Physik*, edited by H. P. J. Wijn (Springer-Verlag, Berlin, 1966), Vol. XVIII.

¹⁵M. E. Lines, Phys. Rev. A **135**, 1336 (1964).